Coupled Preliminary Design and Trajectory Optimization of Rockets using a Multidisciplinary Approach

Fábio Miguel Pereira Morgado
fabio.p.morgado@tecnico.ulisboa.pt

Instituto Superior Técnico, Universidade de Lisboa, Portugal

June 2019

Abstract

A tool was developed to perform a rocket preliminary design by finding the optimal design and trajectory parameters for a specific mission, using a multidisciplinary coupled approach. The design optimization is performed using a developed continuous genetic algorithm, able to perform parallel optimization. The mass and sizing models required to estimate the rocket structure are created using historical data regression or taken from literature. The trajectory optimization is done using the Pontryagin's Minimum Principle. The optimality equations are deduced and the optimal values are found using a particle swarm optimization. The tool is tested by optimizing the design of a small launch vehicle and comparing it to the state-of-the-art rocket. The tool shows promising results in both trajectory and design optimization. It handles the imposed constraints and is able to successfully perform a launch vehicle conceptual design and trajectory calculation in a reasonable time.
Keywords: Coupled approach, Launch vehicle, Trajectory optimization, Genetic algorithm, Particle swarm optimization

1. Introduction

Space companies design new launchers while seeking the minimum cost configuration able to perform a set of reference missions, such as sending a satellite of some mass to orbit. Current technology allied to continuous development of Multidisciplinary Design Optimization (MDO) algorithms is a powerful tool to build cheaper and better rockets.

The design of a rocket is a very challenging activity when safety, reliability and performance are considered. A substantial part of the overall launcher development is committed at the conceptual design phases, and at least 80% of the life-cycle costs are comprised by the chosen design concept [1]. To reduce the complexity and life-cycle cost of space launchers, there is the need to significantly improve early systems analysis capability in the conceptual and preliminary design phase

The design optimization involves the interaction of diverse engineering disciplines which often have conflicting objectives and demand a vast search space to find the global optimum. This requires adapted design multidisciplinary tools which allow to integrate the constraints inherent to each discipline and to ease the compromise search. Traditionally, the Multidisciplinary Feasible (MDF) method is used for rocket optimization, splitting the design problem according to the different disciplines and associating a global optimizer at the system level, while complying with all discipline constraints [2].

The main objective of this work is the creation of an algorithm capable of designing and/or optimizing rockets using evolutionary algorithms, according to the given mission specifications and design variables. This task led to the development of aerodynamic and mass models, as well as a trajectory optimization algorithm. Due the the high computation cost involving the optimization process, the algorithm allows computational parallelization to enhance the process speed.

2. Rocket Fundamentals

2.1. Rocket performance

A mission requires the rocket to achieve a specified velocity to deliver the payload into the desired orbit. Disregarding external forces, the velocity change is determined by the Tsiolkovsky rocket equation

$$\Delta V = V_f - V_0 = v_e \ln \frac{m_0}{m_f}, \tag{1}$$

where ΔV is the maximum change of velocity, v_e the effective exhaust velocity, m_0 the initial rocket mass and m_f the final rocket mass.

In reality, the rocket is subjected to external forces, the most important being drag and gravity, causing energy losses throughout the mission profile. The energy losses may be expressed in terms

of velocity losses, transforming the required mission velocity change into

$$\Delta V = \Delta V_{orbit} + \Delta V_{drag} + \Delta V_{gravity} + \Delta V_{thrust}, \quad (2)$$

where ΔV_{orbit} is the ideal velocity required for the rocket to achieve in order to reach the desired orbit, and ΔV_{drag} and $\Delta V_{gravity}$ are the velocity losses due to drag and gravity, respectively. The term ΔV_{thrust} is the wasted velocity due to steering, so the vehicle can correct its trajectory. By definition, the gravity loss is

$$\Delta V_{gravity} = \int_{t_0}^{t_f} g \sin\gamma \; dt, \quad (3)$$

where g represents the gravitational acceleration and γ the flight path angle. The initial time t_0 and final time t_f are the boundaries of the time interval to calculate the velocity loss, usually comprising the entire flight duration. The drag loss is given by

$$\Delta V_{drag} = \int_{t_0}^{t_f} \frac{D}{m} dt, \quad (4)$$

where D is the drag force, and m the rocket mass. The velocity loss induced by steering is

$$\Delta V_{thrust} = \int_{t_0}^{t_f} \Big(\frac{T}{m} - \frac{T}{m} \cos\chi \Big) dt, \quad (5)$$

where χ is the angle between the velocity vector and thrust vector, and T is the rocket thrust at the given time. A reasonable preliminary estimation is considering the losses typically between 1.5 to 2 km/s, predominantly due to gravity.

Rocket thrust is a result of the change of the gas momentum due to the transformation of heat into kinetic energy, defined as

$$T = \dot{m} V_e + A_e (P_e - P_a), \quad (6)$$

where $\dot{m}$ is the mass flow rate through the nozzle, V_e the exhaust velocity, A_e the exit nozzle area, and P_e and P_a the exit nozzle pressure and atmospheric pressure, respectively.

To compare different propellants and engines, the specific impulse parameter is used. It has units of second, describing the total impulsed delivered per unit weight of propellant, given by

$$I_{sp} = \frac{T}{\dot{m} g_0} = \frac{v_e}{g_0}, \quad (7)$$

where $g_0 = 9.80665 \; m/s^2$ is the acceleration of gravity at the Earth's surface.

2.2. Staging

Staging allows the vehicle not to transport all the structure to orbit, thus saving propellant and reducing the rocket mass. In serial staging, the stages are stacked upon each other and the thrust is provided by one stage at a time. When the propellant depletes, the engines are turned off and the stage discarded from the rocket, reducing the dead weight.

For a N-stage rocket, the kth stage mass is given as

$$m_k = m_{p,k} + m_{s,k}, \quad (8)$$

where m_s represents the structural mass and m_p the propellant mass.

To ease the rocket analysis, it is common the use of dimensionless mass ratios. The structural ratio is a dimensionless measure of how much of the stage mass is structural. The stage structural mass comprises only the dry mass, and the structural ratio of the kth stage is defined as

$$\sigma_k = \frac{m_{s,k}}{m_k}. \quad (9)$$

For a multi-stage rocket with a total of N stages, the ideal velocity increments is the sum of the individual stage contribution. The Tsiolkovskys rocket equation (1) can be rewritten as

$$\Delta V = \sum_{k=1}^{N} v_{e,k} \ln \frac{m_{0,k}}{m_{f,k}}, \quad (10)$$

where $m_{0,k}$ is the sum of the k_{th} stage mass and payload mass, and $m_{f,k}$ is the sum of the k_{th} stage structural mass and payload mass.

2.3. Trajectory

Space launchers have to reach a specific orbit to deliver the desired payload, which is done by following an ascent trajectory path, typically following the steps in figure 1. The trajectory path has a major influence in the design and performance of the launch vehicle, and if not optimized, it may have significant effects on the maximum payload mass allowed to orbit.

The majority of space launch vehicles take off from the ground launch pad and tries to leave atmosphere as soon as possible to reduce drag losses. However, a steep ascent leads to more gravity losses as more energy is required to overcome gravity. Hence, the vehicle performs a pitch over maneuver after tower clearance, starting the gravity turn maneuver.

The use of a gravity turn allows the vehicle to maintain a practically null angle of attack throughout the atmosphere, while it accelerates through the maximum dynamic pressure zone, minimizing the transverse aerodynamic stress.

The gravity turn maneuver ends when dynamic pressure becomes negligible, the shroud protecting

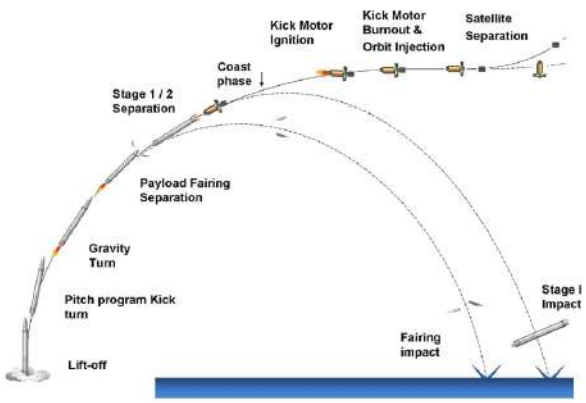

Figure 1: Typical flight sequence of a space launch vehicle.

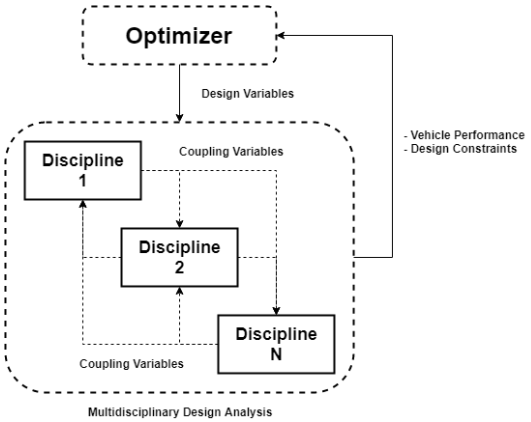

Figure 2: Scheme of the Multidisciplinary Design Feasible method [3].

the payload is dropped off and the rocket starts correcting trajectory, starting the free-flight phase.

Typically, during this phase, the rocket tries to gain enough velocity to perform a coast to the final orbital altitude by reducing the flight path angle, decreasing the gravity losses, and by consuming the propellant as fast as possible, to reduce mass. Afterwards, the rocket is injected into the specified orbit by restarting the engine, which will provide a small impulse, ideally as short as possible.

3. Rocket Design and Optimization

Designing a launch vehicle involves several engineering disciplines, namely, aerodynamics, propulsion, structure, weight and sizing, costs and trajectory. The use of MDO methods allows the combination of the design variables and trajectory optimization, making it suitable for space launchers design.

3.1. MDO Application to Launch Vehicle

The most used MDO method for general design optimization is the MDF method, illustrated in figure 2. The MDF uses a single-level optimization formulation, requiring only one optimizer at the system-level and a Multidisciplinary Design Analysis (MDA) to solve the interdisciplinary coupling equations at each iteration of the optimization process, typically using the Fixed Point Iteration (FPI) method.

The disciplines are analyzed sequentially due to the coupling between downstream and upstream disciplines. At the end of each iteration, the optimizer evaluates the design performance and verifies if the design complies with the given constraints. A feasible solution is produced at each iteration.

3.2. Optimization Algorithms

Over the last two decades, there has been an increasing interest in heuristic approaches, which are typically inspired by natural phenomena and are well suited for discrete optimization problems. The Genetic Algorithm (GA) and Particle Swarm Optimization (PSO) have been widely used in space industry for both design and trajectory optimization.

The GA is inspired in Darwins theory of evolution, by the inclusion of selection, crossover and mutation techniques. They are useful to solve engineering design problems, presenting the ability to combine discrete, integer and continuous variables, no requirement for an initial design, and the ability to address non-convex, multi-modal and discontinuous functions. A continuous GA was developed to optimize the rocket design, allowing an easy implementation and parallel optimization.

The PSO algorithm models the social behavior of animal groups, using information obtained from each individual and from the swarm to reach the optimum solution. It was chosen to optimize the rocket trajectory, as it allows to accurately calculate the required trajectory path using indirect methods [4], while minimizing the propellant consumption and the rocket total mass.

3.3. Trajectory Optimal Control

To find the rocket optimal control, direct and indirect methods can be used. In general, direct methods are more robust, but provide less accurate results, critical for aerospace application. The indirect methods are harder to initialize, but a PSO can be implemented to search the optimal trajectory parameters.

Indirect methods use the theory of optimal control to transform the optimization problem into a Two Point Boundary Value Problem (TPBVP) by introducing adjoint variables. The adjoint variables, the control equation and the boundary conditions (transversality conditions) have to be analytically deduced and solved, in compliance with the Pontryagins Maximum Principle (PMP).

These equations are deduced from the Hamilto-

nian function given as

$$H = \lambda^T f + L, \tag{11}$$

where $\lambda^T f$ is the adjoint variables conjugate to the state equations, and L is the Lagrangian of the system. The adjoint differential equations are deduced using

$$\frac{d\lambda}{dt} = -\Big(\frac{\partial H}{\partial x}\Big)^T, \tag{12}$$

where x represent the state variables.

The optimal control is determined by minimizing the Hamiltonian with respect to the control variables u,

$$\Big(\frac{\partial H}{\partial u}\Big)^T = 0, \tag{13}$$

and by assuring the Legendre-Clebsch condition ($\frac{\partial^2 H}{\partial u^2}$ has to be positive semidefinite).

Finally, the transversality conditions can be deduced by solving

$$(\Phi_t + H)|_{t=t_f} = 0, \tag{14}$$

where Φ is the boundary condition function, given by

$$\Phi = J + \nu^T \Psi(x_f), \tag{15}$$

being J the objective function, and $\nu^T \Psi$ is the time-independent adjoint variable conjugate to the imposed boundary conditions.

The method tries to minimize the objective function, while complying with the optimality constraints. Common objectives are the time of flight and the propellant consumption.

4. Optimal Rocket Design Procedure

The construction of the models integrated in the algorithm, together with the algorithm itself, are explained in this section. The disciplines are divided in modules, that can be replaced by higher-fidelity models in the future, improving the accuracy of the solution.

4.1. Dry Mass Estimation and Sizing

For a liquid engine, the mass is the sum of the system components as [5]

$$m_{LE} = m_{tc} + m_{tankO} + m_{tankF} + m_{st}, \tag{16}$$

where m_{tc}, m_{tankO}, m_{tankF} and m_{st} are the masses of the the thrust chamber, oxidizer tank, fuel tank, and support structure, respectively.

The thrust chamber is composed by the propellant injectors, igniter, a combustion chamber, an exhaust nozzle and a cooling system. The mass can be estimated by

$$m_{tc} = \frac{T}{g_0(25.2\log(T) - 80.7)}. \tag{17}$$

To calculate the support structure mass, an empirical equation is used,

$$m_{st} = 0.88 \times 10^{-3} \times (0.225T)^{1.0687}. \tag{18}$$

The tanks were assumed to be cylindrical tanks with semi-spherical ends. The mass of the tank is calculated by

$$m_{tank} = (A_c \times th_c + A_s \times th_s) \times \rho_{mat}, \tag{19}$$

where ρ_{mat} is the material density, A_c and A_s are the surface area of the cylindrical and spherical sections, respectively, and th_c, th_s the wall thickness. The thickness is calculated relatively to the burst pressure, given as

$$P_b = \eta_s \lambda_b (10^{-0.10688(\log(V_{tank}) - 0.2588)}) \times 10^6, \tag{20}$$

where V_{tank} is the tank volume required to store the propellant. A safety factor η_s equal to 2, and a ratio between the maximum expected operating pressure and the tank pressure λ_b equal to 1.2 are used, as recommended in [5].

The stage inert mass has to account the outer-shell, given as

$$\begin{aligned} m_{Stage} =& m_{LE} + \rho_{mat} L_{stage} \\ & \times \pi \left[\frac{D_{stage}^2}{4} - \Big(\frac{D_{stage}}{2} - th\Big)^2 \right], \end{aligned} \tag{21}$$

where m_{LE} is the liquid engine mass, th is the thickness of the wall and L_{stage} and D_{stage} are the stage length and diameter, respectively.

The length of the liquid stage is calculated as the sum of the tanks and thrust chamber lengths [5],

$$L_{LS} = L_{tc} + L_{tankO} + L_{tankF}, \tag{22}$$

where L_{tc} is the thrust chamber length and L_{tankO}, L_{tankF} are the oxidizer and fuel tank lengths, respectively. The thrust chamber length is calculated using

$$L_{tc} = 3.042 \times 10^{-5} T + 327.7. \tag{23}$$

The tank length is determined by

$$L_{tank} = D_{tank} + \frac{V_{tank} - \frac{4}{3}\pi(\frac{D_{tank}}{2})^3}{\pi(\frac{D_{tank}}{2})^2}, \tag{24}$$

4.2. Trajectory Model

The trajectory was divided in different flight phases comprising of vertical ascent, pitch over, gravity turn and free flight phase. The pitch over maneuver will simply be represented as a small discontinuity step in the flight path angle. After the gravity turn, the trajectory optimization is solved by defining an Hamiltonian function and applying the PMP, using a PSO algorithm to explore the search space for the optimal solution of the problem.

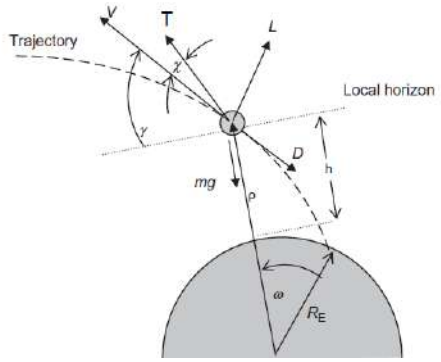

Figure 3: Rocket state variables and forces during flight [6].

The rocket is assumed to be a variable-mass rigid body flying in a 2-D plane model, as illustrated in figure 3. The forces acting in the rocket are applied at the center of mass during flight.

The rocket's active stage produces a thrust T with an angle χ in respect to the velocity vector V. In the context of trajectory analysis and optimization, the thrust direction can be assumed as always aligned to the vehicle longitudinal axis ($\chi \equiv \alpha$).

The force of gravity applied on the vehicle is mg, where m is the vehicle mass and g the local gravitational acceleration, which points to the center of the Earth at all times.

The aerodynamic drag force D is given as function of the vehicle flight speed V, the mass density ρ and a characteristic surface area S, as

$$D = C_D \frac{1}{2} \rho S V^2, \tag{25}$$

where C_D is the drag coefficient.

The lift force L is neglected as it is held closely to zero during the powered ascent through the atmosphere. The Coriolis and centripetal acceleration due to the Earth rotation are also neglected during trajectory simulation. The contribution due to Earth rotation is taken into consideration before the start of the simulation. A reference system that rotates with the Earth and has the origin in its center, is used to better describe the rocket motion.

The equations of motion for the tangential and normal direction, respectively, are

$$\dot{V} = \frac{T}{m} \cos \alpha - \frac{D}{m} - g \sin \gamma \tag{26}$$

and

$$V\dot{\gamma} = -\Big(g - \frac{V^2}{R_e + h}\Big) cos\gamma + \frac{T}{m} \sin \alpha, \tag{27}$$

where $R_e = 6.371 \times 10^6$ m is the radius of the earth and h is the vehicle altitude.

The equations for downrange distance x and altitude h are

$$\dot{x} = \frac{R_e}{R_e + h} V \cos \gamma \tag{28}$$

and

$$\dot{h} = V \sin \gamma. \tag{29}$$

To avoid transversal aerodynamic loads, α is held null until the termination of the gravity turn. Afterwards, better trajectories are enabled by deflecting the thrust, starting the free-flight phase. The free flight phase can be treated as a TPBVP, in which the vehicle initial position corresponds to the end of gravity turn and the final position to the insertion in the specified orbit.

The optimal controls for the optimized trajectory are found by applying the PMP and the boundary value problem is then solved by using a shooting method to find the Lagrangian multipliers. The proposed method is an extension of the work performed in [4].

The problem objective is to reduce the propellant consumption, which is equivalent to minimize the thrusting time. The proposed objective function is to reduce the final impulse time to reach circular orbit, expressed as

$$J = t_f - t_{cf}, \tag{30}$$

where t_f and t_{cf} are the final flight time and the final coast time, respectively.

The flight arcs are divided by the discontinuities in mass and thrust through the flight. The terminal boundary constraints are

$$\boldsymbol{\Psi} = \begin{bmatrix} \Psi_1 \\ \Psi_2 \\ \Psi_3 \end{bmatrix} = \begin{bmatrix} h_f - h' \\ V_f - V' \\ \gamma_f - \gamma' \end{bmatrix} = 0, \tag{31}$$

where h', V', and γ' are the final state values, for the vehicle to reach the desired orbit. The final time t_f and final downrange x_f are unknown.

The Hamiltonian for each flight arc is set as

$$H = L + \boldsymbol{\lambda}^T \boldsymbol{f} = \lambda_x \dot{x} + \lambda_h \dot{h} + \lambda_V \dot{V} + \lambda_\gamma \dot{\gamma}, \tag{32}$$

and the boundary condition function as

$$\Phi = J + \boldsymbol{\nu}^T \boldsymbol{\Psi}(x_f) \implies (t_f - t_{cf}) + \boldsymbol{\nu}^T \boldsymbol{\Psi}(x_f), \tag{33}$$

where $\boldsymbol{\lambda}$ is the adjoint or costate variable conjugate to the state equations and $\boldsymbol{\nu}$ is the time-independent adjoint variable conjugate to the boundary conditions. Due to the Weierstrass-Erdmann corner conditions, the adjoint variables are continuous across successive flight arcs.

To minimize the Hamiltonian, the set of conditions that need to be satisfied are

$$\dot{\lambda}_x = 0, \tag{34a}$$

$$\dot{\lambda}_h = \frac{1}{(Re+h)^2} V\lambda_\gamma \cos(\gamma) - \Big(2\mu_E\lambda_V \sin\gamma + \frac{2\mu_e\lambda_\gamma\cos\gamma}{V}\Big)\frac{1}{(R_E+h)^3}, \tag{34b}$$

$$\dot{\lambda}_V = -\lambda_h \sin\gamma - \lambda_\gamma\Big[\cos\gamma\Big(\frac{1}{R_E+h} + \frac{\mu_E}{(R_E+h)^2V^2}\Big) - \frac{T}{m}\frac{1}{V^2}\sin\alpha\Big], \tag{34c}$$

$$\dot{\lambda}_\gamma = -V\lambda_h\cos\gamma + \mu_E\lambda_V\frac{\cos\gamma}{(R_E+h)^2} + \lambda_\gamma\sin\gamma\Big(\frac{V}{(R_E+h)} - \frac{\mu_E}{(R_E+h)^2V}\Big). \tag{34d}$$

Recognizing the costate equations (equation (34)) as homogeneous in λ, the costate initial values can be sought in the interval $-1 \leq \lambda_k \leq 1$, reducing the search space.

For the optimization problem, the control variable used is the thrust deflection χ, which can be written in terms of the adjoint and state variables through the Pontryagin's Minimum Principle,

$$\alpha = \arg\min_{\alpha} H, \tag{35}$$

which is the equivalent to solve

$$\frac{\lambda_\gamma}{V}\sin\alpha + \lambda_V\cos\alpha = 0, \tag{36}$$

with $\sin\alpha = -\frac{\lambda_\gamma}{V}\sqrt{\Big[\big(\frac{\lambda_\gamma}{V}\big)^2 + \lambda_V^2\Big]}$ and $\cos\alpha = -\lambda_V\sqrt{\Big[\big(\frac{\lambda_\gamma}{V}\big)^2 + \lambda_V^2\Big]}$ to verify the PMP.

The coast time and the burn time of the last stage are unspecified. Hence, the transversality condition is given by

$$H_f^{\text{last stage}} + H_f^{\text{coast}} - H_0^{\text{last stage}} = 0, \tag{37}$$

with $H_f^{\text{last stage}} < 0$.

The use of the penalty function allows to deal with trajectory contraints, by building a single objective function, able to be minimized by the PSO algorithm. The new objective function is expressed as

$$J' = J + \sum_{c=1}^{3} \boldsymbol{s}_c||\boldsymbol{x}_{c,f} - \boldsymbol{x}'_c|| + s_4||H_f^{\text{last stage}} + H_f^{\text{coast}} - H_0^{\text{last stage}}||, \tag{38}$$

where s_c denotes the constraint weighting factor, $\boldsymbol{x}_f$ the final state vector and $\boldsymbol{x'}$ the required state vector. The original objective function J is penalized if the rocket does not reach the required altitude, velocity or flight path angle and if the transversality condition is not verified.

4.3. Algorithm Development

A continuous GA was built to handle the optimization process with a parallelization option based on the master-slave architecture, shown in figure 4. The master node scatters the population individuals throughout the slave nodes, which perform the individual evaluation to assess the fitness and return the information to the master node to create a new generation.

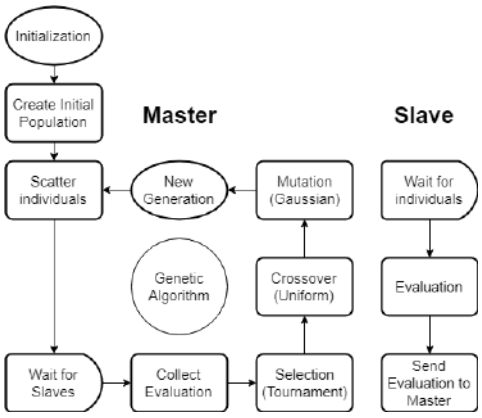

Figure 4: Genetic Algorithm implementation using master-slave architecture.

The benchmark of the GA was performed by using DEAP's GA as comparison, showing reasonable results. The population initialization is performed using a maximin latin hypercube method, maximizing the smallest distance between any two design points, spreading them evenly over the entire design region. The parents are selected through tournament, followed by an uniform crossover and a Gaussian mutation, creating the children for the next generation. After testing, the chosen crossover rate and mutation rate were $p_c = 0.75$ and $p_m = 0.5e^{-0.025gen_k}$, where gen_k is the generation number. The chosen step-size for the Gaussian mutation is $\lambda = 1.0e^{-0.075gen_k}$.

The evaluation module can be divided in two blocks: rocket construction block, where the mass and sizing of the rocket is calculated, and the trajectory optimization block, where the optimal trajectory is calculated using the PyGMO PSO algorithm. After each block, the algorithm verifies the constraints, penalizing the objective function if they are violated.

Firstly, the algorithm proceeds to calculate the mass and dimensions of the rocket using the mass model. The mass model calculates the stages propellant and inert masses and dimensions sequentially, starting by the last stage. This is an itera-

tive process, as adding structural mass requires an increase of propellant mass to achieve the desired ΔV. The loop ends when the structural factor converges, progressing to the next stage.

Before starting the trajectory optimization, the design constraints are checked for violations. If any constraint is violated, the rocket mass suffers a penalty and the individual evaluation ends without performing the trajectory simulation. The design constraints implemented are $1.2 \leq TWR \leq 2$ at lift-off, with TWR representing Thrust-to-Weight ratio, and 8500 m/s $\leq \Delta V \leq$ 10000 m/s. Both constraints allow to diminish the search space, thus facilitating the search for feasible designs.

The trajectory model uses a fourth order explicit Runge-Kutta method (RK4) to generate the numerical trajectory solution. The PSO algorithm provides the trajectory parameters needed to find the optimal path. A trajectory simulation is performed for each particle created by the PSO, until the rocket reaches orbit or when the maximum number of iterations is reached. Each particle is initiated with a parameter set represented by the unknown initial costate values $(\lambda_{0h}, \lambda_{0V}, \lambda_{0\gamma})$, the coast duration Δt_c and initialization time t_{ic}, last stage duration Δt_T and the pitch angle γ_p for the pitch maneuver.

During the gravity turn and free flight, the stages burn time and acceleration are monitored. The algorithm limits the rocket acceleration when using liquid stages ($a \leq 5g_0$) to protect the payload by throttling down the engines. When the propellant tank is depleted, staging occurs. The condition chosen to end the gravity turn was the aerothermal flux to reach a value below 1135 W/m^2, where the fairing can be jettisoned without warming the payload. The aerothermal flux is evaluated using

$$\phi = \frac{1}{2}\rho V^3. \tag{39}$$

Afterwards, the optimal control, given by the costate variables, is initiated. The rocket continues to thrust until the start of the coast phase, which only occurs during the last stage thrusting. The stage then proceeds to burn until the burn time Δt_T is reached.

Finished the trajectory optimization, the algorithm verifies if the rocket has successfully reached orbit. Thus, the algorithm verifies if buckling is on eminence, using a safety factor of 1.5, and if the maximum dynamic pressure affecting the rocket surpasses the maximum admissible value ($q \leq$ 55000 N/m^2), penalizing the mass if the constraints are violated.

For a thin elastic cylindrical shell of radius R, thickness th, and Young modulus E, the linearized buckling equations, the critical stress is given by [7]

$$\sigma_{crit} = \frac{E}{\sqrt{3(1-\nu^2)}}\Big(\frac{th}{R}\Big), \tag{40}$$

where ν is the material Poisson's ratio. For an aluminum-alloy, $\nu = 0.32$.

5. Preliminary Design of a Small Launch Vehicle

In the remark of testing how well the tool designs a rocket, a small-LV optimization design is conducted using an Electron's reference mission [8], allowing to compare the characteristics of the obtained rocket and the Electron rocket.

5.1. Algorithm Setup

The optimization will focus only on two-stage and three-stage rockets. The considered mission is shown in table 1.

Payload Mass [kg]	150
Altitude [m]	500000
Velocity [m/s]	7612
Flight Path Angle [rad]	0.0

Table 1: Mission specification.

The trajectory optimization parameters are shown in table 2. To prevent lack of propellant due to engine malfunction, the maximum value for the last stage duration is 95%, leaving 5% of propellant as reserve.

	PSO Boundary Range
Coast Time [s]	500 - 4000
Pitch Angle [rad]	1.55 - 1.57
Adjoint Variables	-1 - 1
Last Stage Duration [%]	70 - 95
Coast Initialization [%]	0 - 100

Table 2: Trajectory parameters for optimization.

The propulsive parameters are specified in table 3. For a better comparison between the optimized rockets and the Electron, the propellant used and the specific impulse are unchanged. Each stage will only have one propulsive engine, reducing the design space.

The design parameters are shown in table 4. The diameter and wall thickness will be equal for all stages. The material chosen for both tank walls and for the rocket walls was the aluminum alloy, with ρ_{mat}=2700 kg/m^3.

	First Stage	Remaining Stages
TWR	1.2 - 2.0	0.8-1.5
Isp [s]	303	333
Nozzle Diameter [m]	$0.6D_{stage}$	$0.9D_{stage}$
Fuel Density [kg/m^3]	810	810
Oxidizer Density [kg/m^3]	1142	1142
O/F Ratio	2.61	2.61

Table 3: Propulsive and propellant parameters.

	Two Stage	Three Stage
Rocket Type	liquid	liquid
ΔV/Stage [m/s]	3000 - 6000	2000 - 4000
Diameter [m]	1.0 - 1.5	1.0 - 1.5
Wall thickness [mm]	2.0 - 5.0	2.0 - 5.0
Engines per Stage	1	1

Table 4: Design Parameters.

The parameters of both GA and PSO optimization algorithms illustrated in table 5 and table 6, respectively. The step-size is normalized with the boundary width.

Maximum Generation	35
Number of Individuals	50
Crossover Rate	0.75
Mutation Rate	$0.5e^{-0.025gen_k}$
Step-Size	$1.0e^{-0.075gen_k}$

Table 5: Genetic algorithm parameters.

Maximum Generation	250
Number of Particles	100
Cognitive Parameter	2.05
Social Parameter	2.05
Inertia Weight	0.7298

Table 6: Particle swarm optimization parameters.

5.2. Results

The algorithm took 9641 seconds to find the optimal two-stage rocket design and 7370 seconds to find the optimal three-stage rocket design. The task was parallelized using a cluster with 13 Intel Xeon E312xx (Sandy Bridge) processors, 4 cores each. Each core has a frequency value of 2000 MHz.

The algorithm convergence is illustrated in figure 5. The algorithm was able to converge within the maximum number of generations.

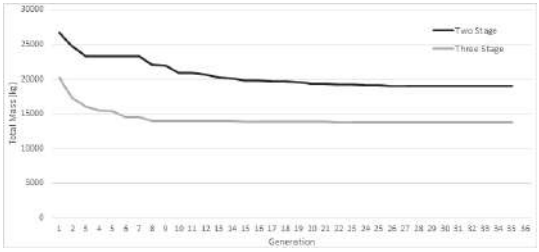

Figure 5: Rockets best total mass evolution.

The optimal design parameters of the two-stage and three-stage rockets are shown in table 7 and table 8, respectively.

	1st Stage	2nd Stage
Delta-V [m/s]	4152	5334
TWR	1.68	1.07
Thickness [mm]	2.01	2.01
Diameter [m]	1.05	1.05
Propellant Mass [kg]	14271	2515
Inert Mass [kg]	1574	383
Fairing Mass [kg]	73	
Total Mass [kg]	18971	

Table 7: Two-stage rocket optimal design parameters

	1st Stage	2nd Stage	3rd Stage
Delta-V [m/s]	3123	3255	2861
TWR	1.80	1.02	0.82
Thickness [mm]	2.01	2.01	2.01
Diameter [m]	1.00	1.00	1.00
Propellant Mass [kg]	8938	2272	554
Inert Mass [kg]	1205	379	177
Fairing Mass [kg]		70	
Total Mass [kg]		13744	

Table 8: Three-stage rocket optimal design parameters

The algorithm was able to handle the design constraints. As expected, the three-stage rocket is a better alternative to the two-stage rocket, drastically reducing the total mass by 5 tonnes. The wall thickness and diameter tend to the minimum boundary value.

	Two Stage	Three Stage
Coast Time [s]	2734	2977
Pitch Angle [rad]	1.566	1.560
Adjoint Variable λ_h	-9.95e-04	-9.97e-04
Adjoint Variable λ_V	-7.79e-01	-1.89e-01
Adjoint Variable λ_γ	-8.88e-01	-8.35e-01
Last Stage Duration [%]	95.0	95.0
Coast initialization [%]	98.8	98.3

Table 9: Rocket optimal trajectory parameters

The optimal trajectory parameters are shown in

table 9. The last rocket stage burns until it consumes 95% of the available propellant, leaving the remaining 5% as reserve. The coast phase is initialized near the last stage ending time for both rockets. Thus, the last stage provides an optimal impulse to reach circular orbit by using between 1% to 2% of the last stage burn time at the end of the flight.

The rocket altitude evolution with time is illustrated in figure 6. Both rocket configurations reached the required altitude with a time difference of 510 seconds. Before the coast phase, the rockets turn horizontally for a brief moment to increase velocity and reduce gravity losses, observable in figure 8.

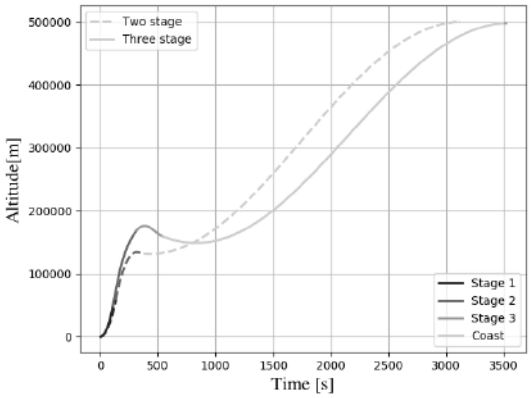

Figure 6: Rocket altitude evolution.

The rocket velocity history is illustrated in figure 7. Once again, both rockets are able to achieve the required velocity for the circular orbit. Before coast phase, both rockets achieve a minimum velocity of 7900 m/s to reach orbit. The two-stage rocket has a faster increase in velocity due to performing staging later.

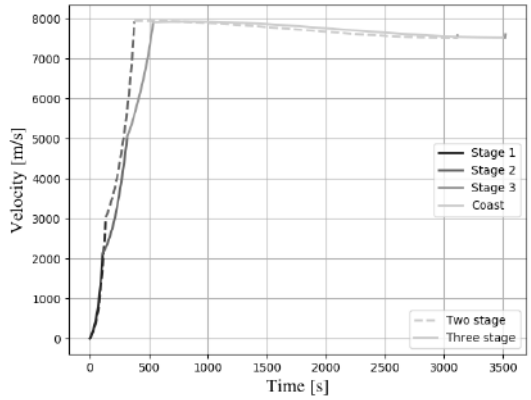

Figure 7: Rocket velocity evolution.

Both rockets have a similar flight path angle evolution in figure 8, that is maintained slightly above zero during the entire coast phase to allow the rocket ascension.

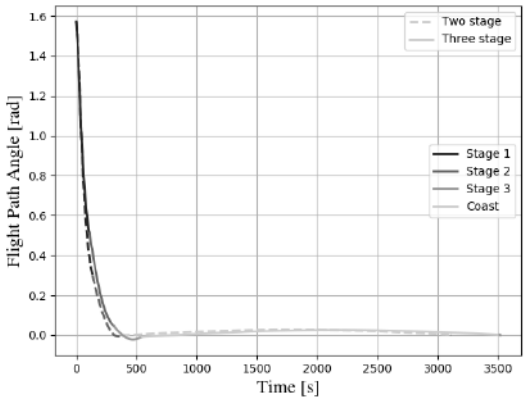

Figure 8: Rocket flight path angle evolution.

The thrust vectoring angle evolution is shown in figure 9. Both rockets have a thrust vectoring angle below 0.2 rad. The control only starts after the fairing jettison, which happens at 188 seconds for the two-stage rocket and at 230 seconds for the three-stage rocket.

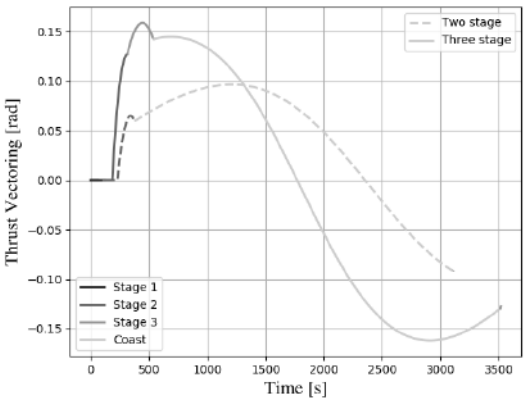

Figure 9: Rocket thrust vectoring evolution.

The constraints, shown in table 10, were successfully handled by the optimizer. The dynamic pressure is below the admissible limit of 55 kPa. Thus algorithm constrains the two-stage rocket acceleration, keeping it below $5g_0$. The axial load for the two-stage rocket and three-stage rocket are below the safety load of 710 kN, suggesting the wall thickness could be further reduced.

Constraint		**Two Stage**	**Three Stage**
Acceleration [m/s^2]	≤ 5.00	5.00	4.72
Dynamic Pressure [kPa]	≤ 55.0	50.5	51.2
Axial Load [kN]	≤ 710	475	390

Table 10: Constrained parameters maximum value.

A comparison between the optimized rockets and the Electron is made in table 11 providing the design. Thus, a simple rocket illustration in figure 10

allows to visualize the dimensions.

	Two Stage Rocket	Three Stage Rocket	Electron Rocket
Number of Stages	2	3	2
Total Mass [kg]	18971	13744	12500
Diameter [m]	1.05	1.00	1.2
Length [m]	22.09	19.12	14.5
Number of Engines	1/1	1/1/1	9/1

Table 11: Comparison of design characteristics between optimized and Electron rocket.

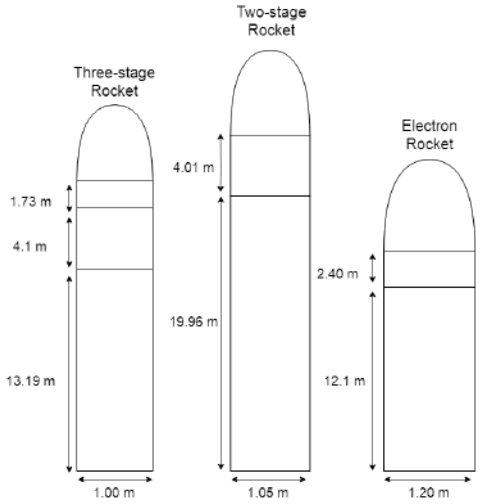

Figure 10: Optimized rockets and Electron rocket dimensions.

The two-stage optimized rocket presents a 52% increase in total mass and length relatively to the Electron rocket, while the three-stage optimized rocket presents only a 10% increase in total mass and a 32% increase in length. The increase in length is not only due to requiring more space for the propellant mass but also because of the smaller diameter.

The larger mass value is not only due to the simplifications made in the dry mass models, but also due to the structural and propulsive assumptions. Regardless of the simplifications made, the tool has proven to be able to successfully optimize rocket design and trajectories using a coupled approach and computational parallelization.

6. Conclusions

In this work a tool capable to perform a rocket preliminary design using a coupled multi-disciplinary optimization approach was developed. Within this framework, a trajectory and staging optimization code were developed separately.

A trajectory model was successfully developed. It is able to find an optimal rocket Pontryagin's Minimum Principle to calculate the optimal control and the PyGMO PSO algorithm to find the optimal trajectory parameters.

The staging optimizer was also able to successfully perform design optimization using the developed GA algorithm, in spite of reducing the total rocket mass. It allowed to perform parallel optimization and was able to converge before the generation limit while successfully handling the imposed design constraints.

The tool is finally tested by performing a two- and three-stage small rocket conceptual design. Both designed rockets are able to perform the mission. Comparatively to the Electron, the three-stage optimized rocket has 10% more mass. The mass and sizing errors are due to the assumptions made, inaccuracy of the mass and sizing models and the use of gravity turn in trajectory.

Nevertheless, the tool is able to perform conceptual rocket design and trajectory optimization, parallelizing the task using a master-slave architecture. The models used by the tool can be replaced independently from the other models to improve the tool in the future.

References

[1] M.-u.-D. Qazi and H. Linshu, "Nearly-orthogonal sampling and neural network metamodel driven conceptual design of multistage space launch vehicle," *Comput. Aided Des.*, vol. 38, pp. 595–607, June 2006.

[2] A. F. Rafique, L. He, A. Kamran, and Q. Zeeshan, "Hyper heuristic approach for design and optimization of satellite launch vehicle," *Chinese Journal of Aeronautics*, vol. 24, pp. 150 – 163, Apr. 2011.

[3] M. Balesdent, *Multidisciplinary Design Optimization of Launch Vehicles*. PhD thesis, Ecole Centrale de Nantes (ECN), Nov. 2011.

[4] M. Pontani, "Particle swarm optimization of ascent trajectories of multistage launch vehicles," *Acta Astronautica*, vol. 94, p. 852864, Feb. 2014.

[5] C. Frank, O. Pinon, C. Tyl, and D. Mavris, "New design framework for performance, weight, and life-cycle cost estimation of rocket engines," 6th European Conference for Aeronautics and Space Sciences (EUCASS), June 2015.

[6] P. Sforza, *Theory of Aerospace Propulsion*. Aerospace Engineering, Elsevier Science, 2011.

[7] W. Tjardus Koiter, *The Stability of Elastic Equilibrium*. PhD thesis, Techische Hooge School, Feb. 1970.

[8] Rocket Lab , *Payload User's Guide*, Apr. 2019.